Supporting Information

Loss of the tumor suppressor BIN1 enables ATM Ser/Thr kinase activation by the nuclear protein E2F1 and renders cancer cells resistant to cisplatin

Watson P. Folk, Alpana Kumari, Tetsushi Iwasaki, Slovénie Pyndiah,
Joanna C. Johnson, Erica K. Cassimere, Amy L. Abdulovic-Cui, Daitoku Sakamuro*

*Correspondence to: dsakamuro@augusta.edu

Supplemental Figures

Fig. S1 Cellular PARylation is enhanced by hydrogen peroxide but is reduced by a PARP inhibitor
Fig. S2 Ectopically expressed BIN1 curbs global poly(ADP-ribosyl)ation, whereas depletion of endogenous BIN1 increases it.
Fig. S3 *In situ* immunofluorescence microscopy confirms that nuclear PARylation, which is increased by hydrogen peroxide, is enhanced further by a BIN1 deficiency.
Fig. S4 Heterologous expression of BIN1 inhibits γH2AX formation with little or no negative effect on cell morphology and cell viability of DU145 cells.
Fig. S5 Expression of si- or sh-BIN1 RNA duplexes effectively and specifically diminishes endogenous BIN1 protein, thereby activating the *ATM* promoter.
Fig. S6 The reduction in BIN1 robustly increases the formation of γH2AX foci in DU145 cells under optimal culture conditions.
Fig. S7 Hob1 (homolog of BIN1) inhibits formation of γH2A foci caused by bleomycin in fission yeast.
Fig. S8 Ectopically expressed BIN1 and BIN1+12A proteins are detected exclusively in the nucleus.
Fig. S9 BIN1 depletion does not upsurge *MRE11A* transcription, but slightly increases the amount of MRE11A protein.
Fig. S10 The formation of γH2AX foci is promoted by the lack of BIN1 irrespective of the status of phosphorylated tyrosine 142 in H2AX
Fig. S11 The formation of γH2AX foci caused by the BIN1 depletion is accompanied by ATM-dependent phosphorylation of MDC1.
Fig. S12 BIN1 deficiency activates the human *PIG3* promoter, a *TP53-inducible Gene-3* promoter.

Supplemental Tables

Table S1 Oligonucleotides used in this study
Table S2 Primary antibodies used in this study
Table S3 si-RNAs and sh-RNAs used in this study
Table S4 Chemicals used in this study

Supplemental References

S1) Pyndiah *et al*, Sci. Signal. **4**, ra19
S2) Lundgaard *et al*, J. Cell. Biochem. **112**, 2992-3001
S3) Routhier *et al*, Oncogene **22**, 637-648
S4) Golding *et al*, Mol. Cancer Ther. **8**, 2894-2902
S5) Polyak *et al*, Nature **389**, 300-305
S6) Okazaki and Sakamuro, J. Cancer Res. Clinc. Oncol. **133**, 581-588

Supplemental Figures

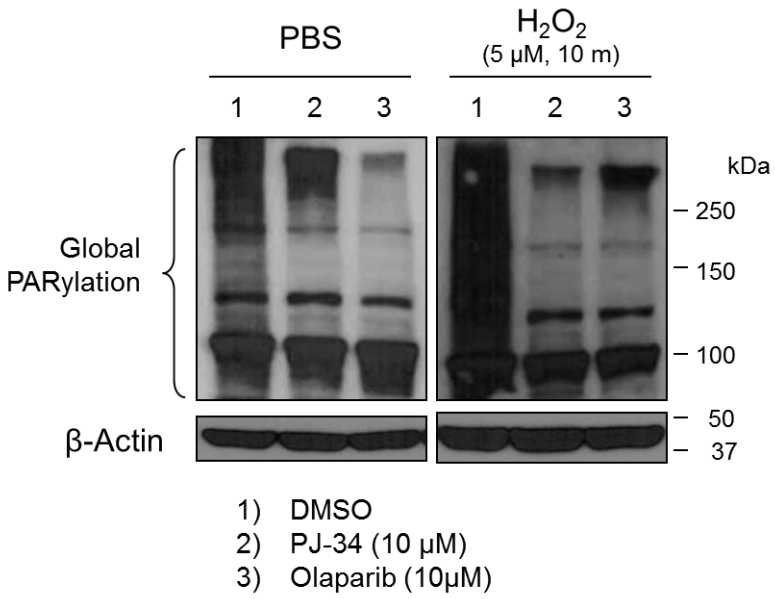

Fig. S1 **Cellular PARylation is enhanced by hydrogen peroxide but is reduced by a PARP inhibitor.**

Actively proliferating DU145 cancer cells were cultured in the presence of the small molecule PARP inhibitors (PJ-34, olaparib) for 4h. Then, cells were treated with hydrogen peroxide (5 μM, 10 min) and the cleared cell lysates were subjected to Western blotting analysis using an anti-PAR antibody. Global poly(ADP-ribosyl)ation (PARylation) was demonstrated by Western blotting analysis probed with an anti-PAR antibody.

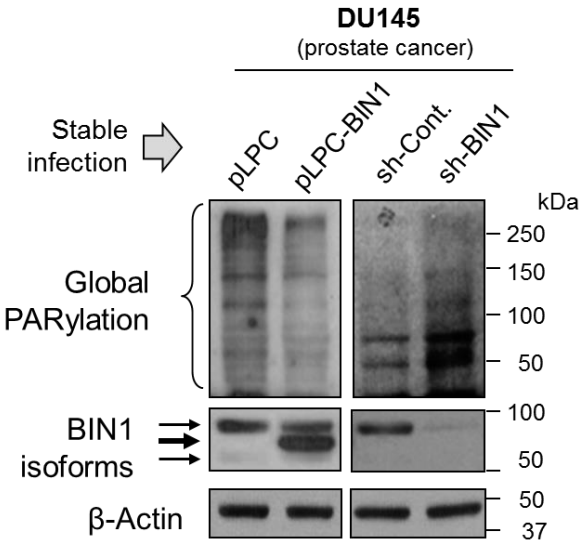

Fig. S2 **Ectopically expressed BIN1 curbs global poly(ADP-ribosyl)ation, whereas depletion of endogenous BIN1 increases it.**

Global poly(ADP-ribosyl)ation (PARylation) was demonstrated by Western blotting analysis probed with an anti-PAR antibody in the human prostate cancer cell line, DU145. Overexpression and depletion of BIN1 were accomplished by stable infection of the pLPC-BIN1 (replication-incompetent) retrovirus and the sh-BIN1-expressing (replication-incompetent) lentivirus, respectively. When BIN1 was overexpressed, the cellular PARylation was prominently reduced. In contrast, the cellular PARylation was apparently increased in BIN1-deficient DU145 cells. We also noticed that the PAR-staining pattern in the pLPC control cell lysates was obviously different from the sh-control cell lysates. This suggests that the efficiency of global PARylation may be somehow controled differently by viral infection.

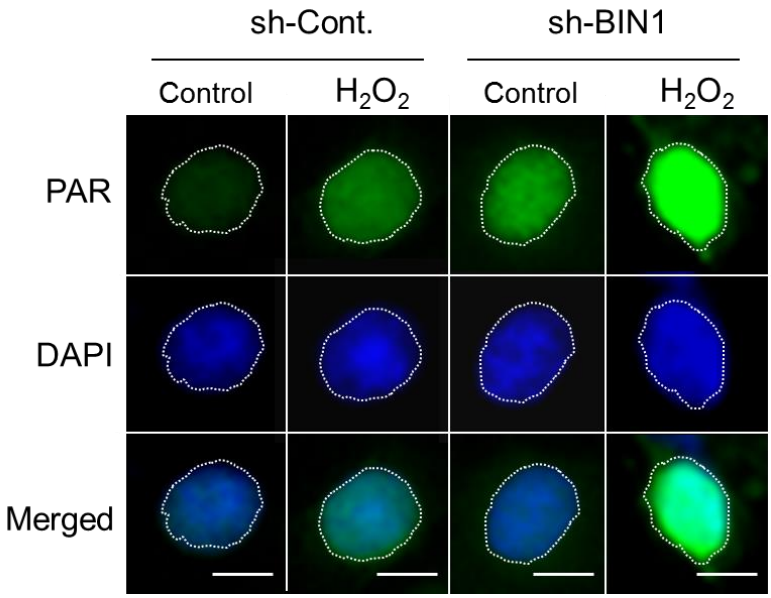

Fig. S3 ***In situ*** **immunofluorescence microscopy confirms that nuclear PARylation, which is increased by hydrogen peroxide, is enhanced further by a BIN1 deficiency.**

In situ immunostaining experiment in actively proliferating DU145 cells demonstrated that the loss of BIN1 increased the PAR-positive signals in the nucleus, which was boosted further by brief treatment with hydrogen peroxide, H_2O_2 (a chemical PARP1 activator). We noticed that the anti-PAR-positive signals in the nucleus that were activated by sh-BIN1 displayed some 'foci-like' morphology. Because BIN1 physically binds PARP1 in the nuclei and inhibits the histone H1 PARylation[S1], this result suggests that BIN1 loss facilitates chromatin remodeling by stimulating the PARylation of histone H1. Nuclei were counterstained with DAPI. Scale bar = 10 μm.

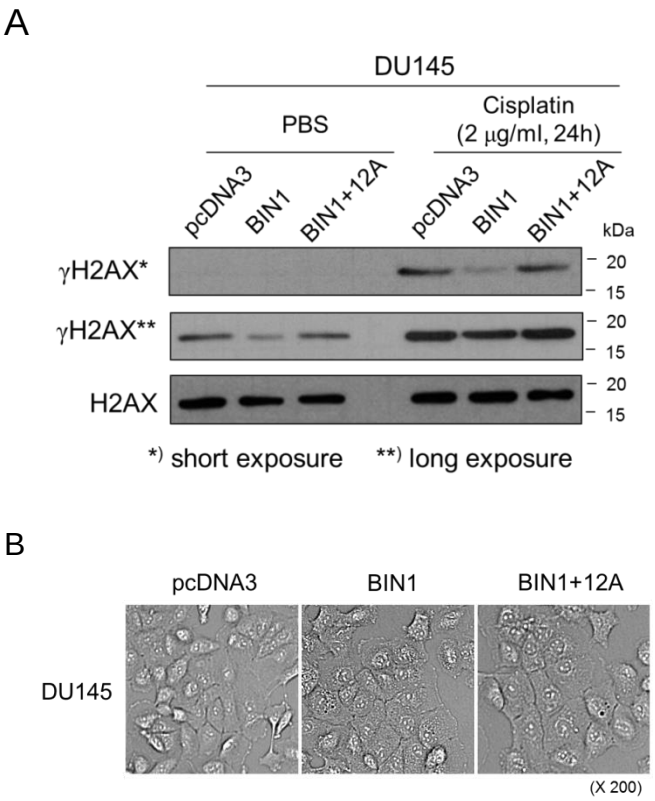

Fig. S4 **Heterologous expression of BIN1 inhibits γH2AX formation with little or no negative effect on cell morphology and cell viability of DU145 cells.**

A) Western blotting analysis demonstrated that ectopically expressed BIN1 consistently suppressed γH2AX formation, even in the presence of cisplatin. However, BIN1+12A did not alter γH2AX formation.

B) Transient transfection of BIN1 and BIN1+12A-expression vectors did not reduce the cell morphology and cell viability. This suggests that the massive reduction in H2AX formation by transfected BIN1 is not attributable to the loss of cell viability.

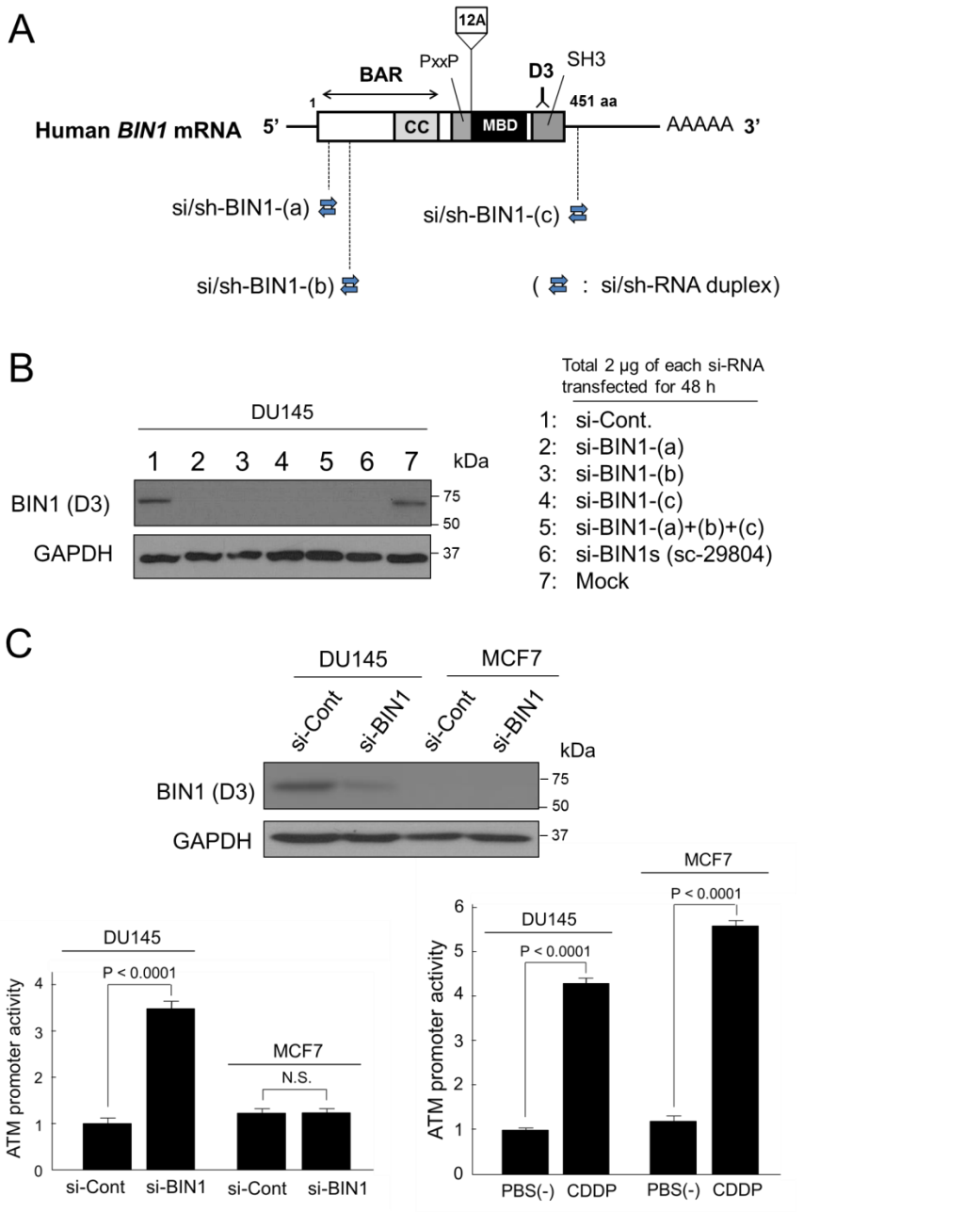

(Continued)

Fig. S5 **Expression of si- or sh-BIN1 RNA duplexes effectively and specifically diminishes endogenous BIN1 protein, thereby activating the *ATM* promoter.**

A) Three different 19-nucleotide sequences (nt) of human *BIN1* mRNA are specifically cleaved by three different si-/sh-BIN1 RNA duplexes (Santa Cruz Biotech., Santa Cruz, CA, USA). Any of these cleavage sites are not subjected to alternative splicing of the human *BIN1* mRNA[S2]. Blast homology search verified that the 19-nt sequence of each si/sh-BIN1 RNA duplex only detects corresponding human *BIN1* mRNA sequence, but not any other *BIN1*-related mRNAs, such as *BIN2*, *BIN3*, and *Amphiphysin I* even under mild homology conditions (data not shown). BAR: BIN-Amphiphysin-Rvs-homologous domain, CC: coiled-coil domain, MBD: MYC-binding

domain, PxxP: proline-x(any amino acid)-x-proline (a possible SH3-binding site), SH3: Src Homology 3 domain.

B) Western blotting analysis probed with an anti-BIN1 monoclonal antibody (clone D3) verified that individual, separate transfection of every single si-BIN1 RNA duplex effectively depleted endogenous BIN1 in DU145 cells. The commercially available mixture of the three si-BIN1 RNA duplex (sc-29804) was used as the positive control. The scramble siRNAs were used as the negative control. GAPDH: glyceraldehyde-3-phosphate dehydrogenase.

C) The transiently transfected si-BIN1 RNA duplexes efficiently increased the 530ATM-luciferase (Luc) activity, which reflects endogenous E2F1 activity (see the main text, **Fig. 4**) in DU145 (BIN1-positive) cells. However, in MCF7 (BIN1-deficient) cells, the si-BIN1 transfection did not release the 530ATM-Luc activity, implying that the si-BIN1 RNA molecule specifically depletes endogenous BIN1. The E2F1 protein per se in MCF7 cells was not dormant because cisplatin (CDDP), which activates E2F1, robustly increased the 530ATM-Luc activity in both DU145 and MCF7 cell lines. PBS(-): phosphate buffered saline, N.S: not significant.

Fig. S5 (*continued*)

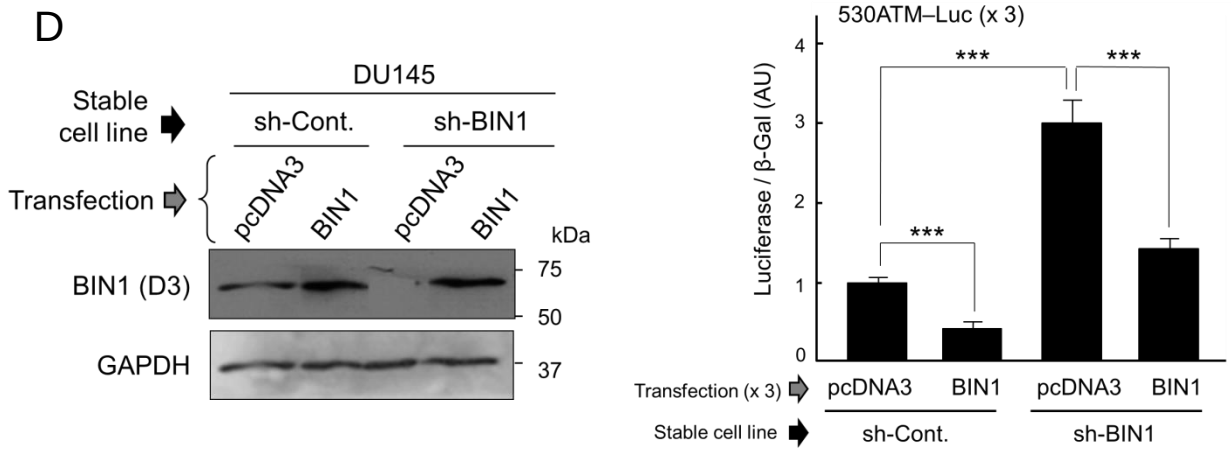

D) In the DU145/sh-Cont(rol) and DU145/sh-BIN1 stable cell lines, which were established by infection of the recombinant sh-control- and sh-BIN1-expressing (replication incompetent) lentiviruses followed by the puromycin selection, the human *ATM* promoter-driven luciferase reporter plasmid vector (530ATM-Luc) was transiently cotransfected with either the pcDNA3 control vector or the pcDNA3-BIN1 expression vector for 48 h. The cleared cell lysates were subjected to Western blotting analysis probed with an anti-BIN1 (D3) monoclonal antibody (*left*) and luciferase assays (*right*). As the internal control to normalize the transfection efficiency for luciferase assays, the pcDNA3-β-galactosidase (β-Gal) expression vector [1/10 (w/w)] was cotransfected. Our result demonstrated that the effect of stable expression of sh-BIN1 on endogenous BIN1 levels was canceled by transiently transfected BIN1 cDNA and that the endogenous E2F1 activity, which was robustly activated by BIN1 depletion (i.e., by sh-BIN1 RNAs), was significantly counteracted by overexpressed BIN1 cDNA.

(x 3): independently transfected three times, ***: $P < 0.001$, AU: arbitrary unit.

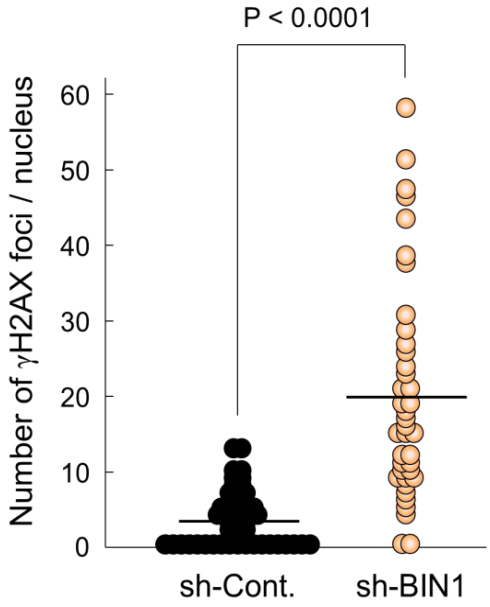

Fig. S6 **The reduction in BIN1 robustly increases the formation of γH2AX foci in DU145 cells under optimal culture conditions.**

In situ immunofluorescence analysis demonstrated that the formation of γH2AX foci detected with an anti-phospho-Ser139 H2AX-specific monoclonal antibody was significantly enhanced in BIN1-depleted DU145 (human prostate cancer) cells. The number of γH2AX foci in the nuclei were counted and plotted. Essentially the same experiment was performed independently three times and the reproducibility was confirmed. The data shown above was a representative one. Horizontal black bars show mean values. Nuclei were counterstained by DAPI.

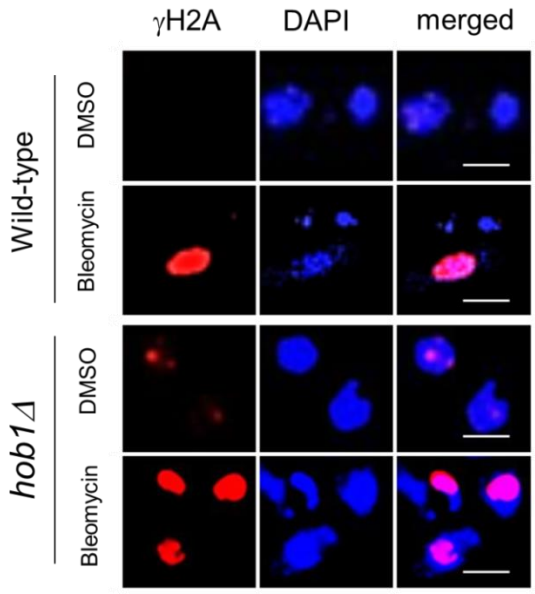

Fig. S7 **HOB1 (homolog of BIN1) inhibits formation of γH2A foci caused by bleomycin in fission yeast.**

Schizosaccharomyces pombe (fission yeast) cells with intact *HOB1* (wild-type) or with *HOB1* deletion (*hob1*Δ)[S3] were treated briefly with bleomycin (40 µg/ml) or di-methyl sulfoxide (DMSO) (1/100 [v/v]) for 2 h and were subjected to *in situ* immunofluorescence analysis probed with an anti-γH2A (yeast H2A phospho-serine 129) antibody. Nuclei were counterstained with DAPI (blue). Scale bar = 2.0 µm.

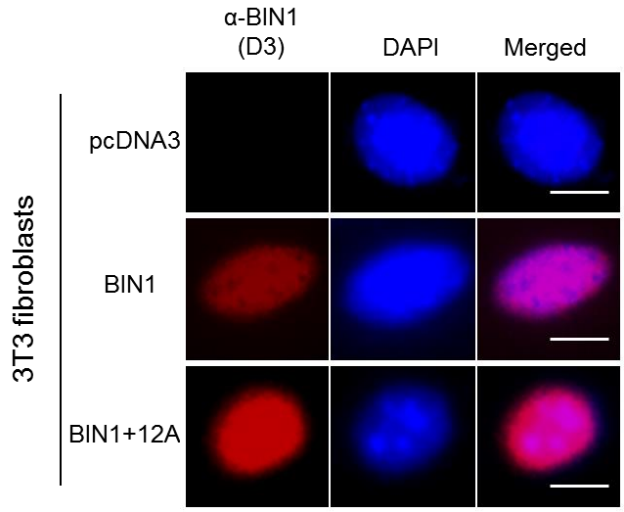

Fig. S8 Ectopically expressed BIN1 and BIN1+12A proteins are detected exclusively in the nucleus.

Mouse 3T3 fibroblasts were transiently transfected with pcDNA3, pcDNA3-BIN1, and pcDNA3-BIN1+12A expression vectors for 48 h. The transfected cells were subjected to *in situ* immunofluorescence analysis. To detect only transfected human BIN1 or BIN1+12A proteins, we used the anti-BIN1 monoclonal antibody (clone D3), which detects all splicing isoforms of human BIN1 protein with little or no cross-reactivity with mouse Bin1 protein (W. P. F and D.S, unpublished observation). Nuclei were counterstained with DAPI (blue). Scale bar = 10 μm.

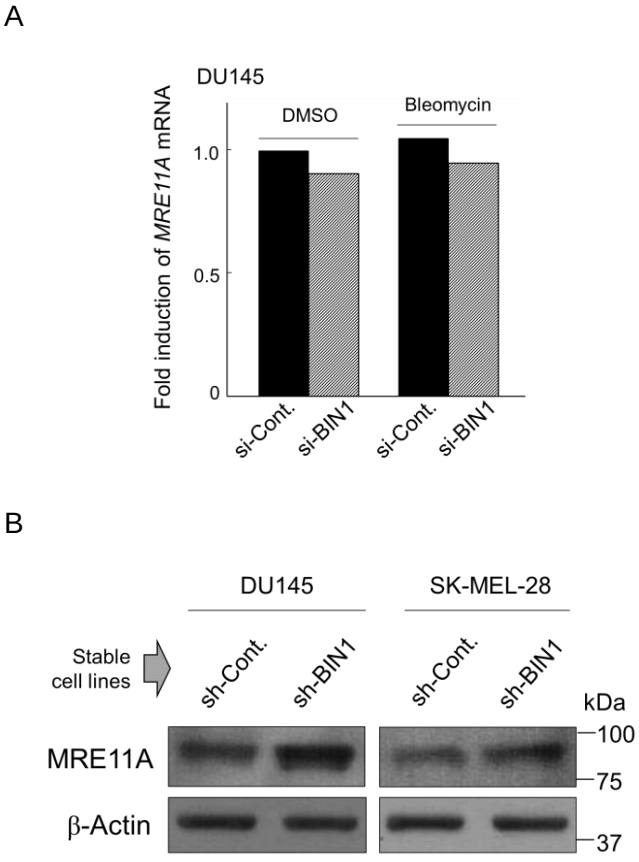

Fig. S9 **BIN1 depletion does not upsurge MRE11A transcription, but slightly increases the amount of MRE11A protein.**

A) qRT–PCR analysis of *MRE11A* mRNA expression in the presence and absence of BIN1. BIN1 loss and bleomycin treatment promptly increase formation of the MRN foci in a transcription-independent manner.

B) Western blotting analysis of MRE11A protein in the presence and absence of BIN1 in the indicated human cancer cell lines. The lack of BIN1 moderately increased the levels of MRE11A. Because the *MRE11A* mRNA is not increased by the BIN1 loss (see [A]), this result suggests that endogenous E2F1 (which is released by BIN1 deficiency) slightly stabilizes the MRE11A protein.

A

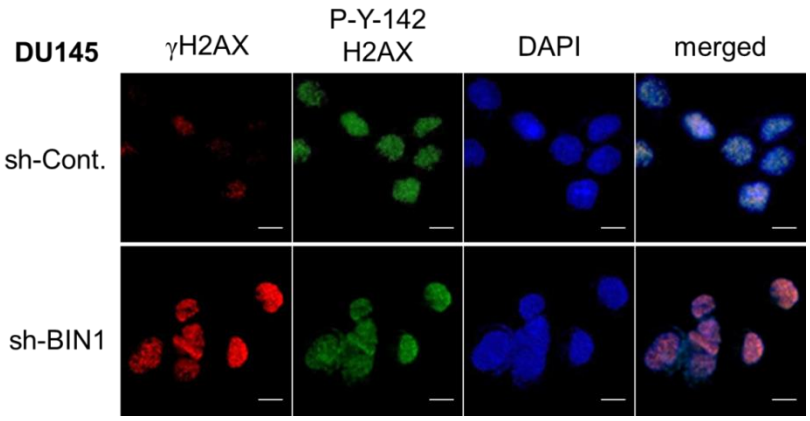

B

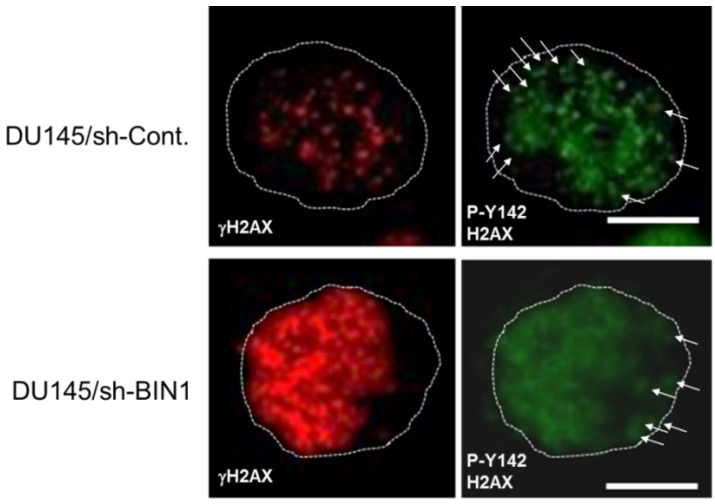

Fig. S10 **The formation of γH2AX foci is promoted by the lack of BIN1 irrespective of the status of phosphorylated tyrosine 142 in H2AX.**

A) *In situ* immunostaining analysis revealed that γH2AX foci (red) robustly increase in the absence of BIN1, whereas phospho-tyrosine 142 H2AX foci (P-Y142 H2AX) (green) are not altered in DU145 cells. Nuclei were counterstained with DAPI (blue). Scale bar = 10 μm.

B) Almost all γH2AX foci are present together with P-Y142 H2AX foci, whereas a certain number of P-Y142 H2AX foci do not exist together with γH2AX foci (white arrows). This suggests that the formation of γH2AX foci after the depletion of BIN1 may not require the dephosphorylation of Y142 in H2AX in advance. White dot lines indicate the boundaries of cell nuclei. Scale bar = 10 μm.

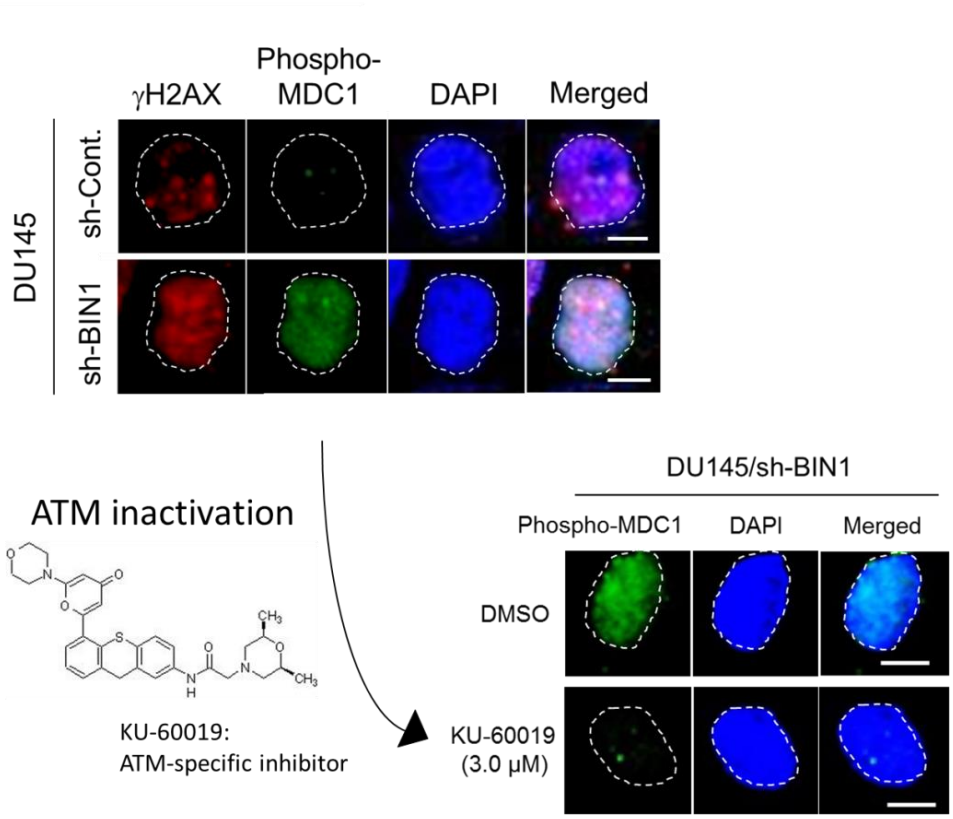

Fig. S11 **The formation of γH2AX foci caused by the BIN1 depletion is accompanied by ATM-dependent phosphorylation of MDC1.**

In situ immunostaining analysis demonstrated that the depletion of BIN1 stimulates the formation of γH2AX foci (red) and phosphorylated MDC1 foci and that MDC1 phosphorylation is diminished by the treatment with KU-60019 (an ATM-specific chemical inhibitor)[S4] at 3.0 μM for 48 h in DU145/sh-BIN1 cells. Nuclei were counterstained with DAPI (blue). Scale bar = 10 μm. Essentially the same *in situ* immunostaining experiment was performed in triplicate and the reproducibility was confirmed.

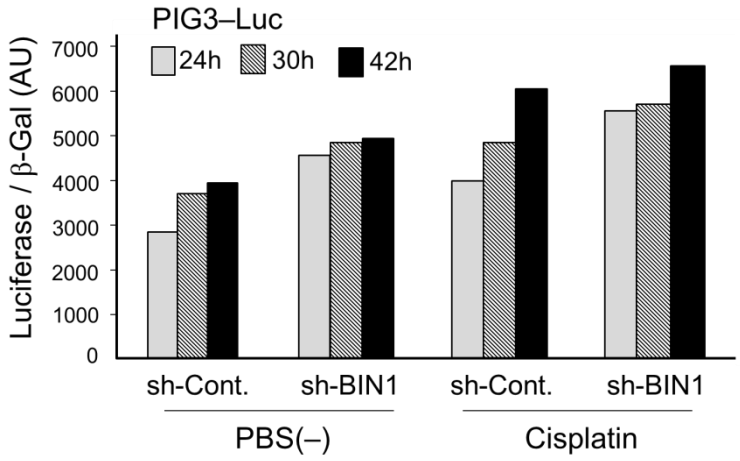

Fig. S12 **BIN1 deficiency activates the human *PIG3* promoter, a *TP53-inducible Gene-3* promoter.**

The PIG3–Luc-transfected LNCaP±pLPC-BIN1 cells were subjected to luciferase assays in the presence and absence of cisplatin (2.0 μg/ml) at 24 h, 32 h, and 42 h. The PIG3–Luc reporter vector is driven by the human *PIG3* (TP53-inducibel proapoptotic gene 3) promoter, a direct target of TP53. The *PIG-3* gene encodes a quinone oxidoreductase homolog, which is involved in TP53-dependent apoptosis[S5] and is directly up-regulated by TP53 in a manner dependent on the TP53 proline-rich region[S6]. AU: arbitrary unit.

Supplemental Tables

Table S1 Oligonucleotide primers used in this study

- *RT-PCR/qRT-PCR primers*

Primer name (F/R)	Nucleotide sequence (5'→3')
Human *ATM* (F)	CAGGGTAGTTTAGTTGAGGTTGACAG
Human *ATM* (R)	CTATACTGGTGGTCAGTGCCAAAGT
Human *MRE11A* (F)	CAGTGTTTAGTATTCATGGCAATCATG
Human *MRE11A* (R)	AATGTCCAAGGCACAAAGTGC
Human *GAPDH* (F)	GAGTCAACGGATTTGGTCGT
Human *GAPDH* (R)	GACAAGCTTCCCGTTCTCAG

(F): forward primer, (R): reverse primer, GAPDH: glyceraldehyde 3-phosphate dehydrogenase

- *ChIP primers*

Primer name (F/R)	Nucleotide sequence (5'→3')
Human *ATM* promoter (–143/–1) (F)	CTTCCGCCAGAGAAAGAAAG
Human *ATM* promoter (–143/–1) (R)	GCTCTCACCCACCCTCTTC
Firefly luciferase (+1053/+1293) (F)	ACACCCGAGGGGGATGATAA
Firefly luciferase (+1053/+1293) (R)	GTGTTCGTCTTCGTCCCAGT

(F): forward primer, (R): reverse primer

- *Sub-cloning primers for the 530ATM/400ATM–Luc vectors*

Primer name (F/R)	Nucleotide sequence (5'→3')
Human *530ATM* (*Xho*I) (F)	CCCCTCGAGGCGACAGCTCCTGCGCCGCATCTCC
Human *ATM* promoter (*Hind*III) (R)*	CCCAAGCTTCCTCTCGCCTCCTCCCGTGGCC
Human *400ATM* (*Xho*I) (F)	CCCCTCGAGGCCCCGCCTCCGTTCGCC
Human *ATM* promoter (*Hind*III) (R)*	CCCAAGCTTCCTCTCGCCTCCTCCCGTGGCC

(F): forward primer, (R): reverse primer, *) The same reverse primer

Table S2 Primary antibodies used in this study

Primary antibody	Purpose	Clone/Catalogue#	Vendor
BIN1 exon 13	WB, IP, ChIP, IF	99D/ sc-13575	Santa Cruz
BIN1 (all isoforms)	WB, IF	D3/ sc-74486	Santa Cruz
BIN1 exon 12A	WB	209-301-E62S	Rockland
E2F1	WB	SAB4500682	Sigma-Aldrich
E2F1	ChIP, WB, IF	C-20/sc-193 X	Santa Cruz
E2F2	WB	H-120/sc-22821	Santa Cruz
E2F3	WB	N-20/sc-879	Santa Cruz
H2AX	WB	07627	EMD
γH2AX	WB, IF	2577S, 05-636	Cell Signaling, EMD
H2A (yeast)	WB	ab13923	Abcam
γH2A (yeast)	WB, IF	ab15083	Abcam
phospho-H2AX (Y142)	WB, IF	ab94602	Abcam
ATM	WB	05-513	EMD
phospho-ATM (Ser1981)	WB, IP, IF	10H11.E12/ sc-47739	Santa Cruz
ATR	WB	N-19/ sc-1887	Santa Cruz
DNA-PKcs	WB	G-4/ sc-5282	Santa Cruz
MDC1	WB	ab114143	Abcam
MDC1 (phospho-T4)	WB, IF	ab35967	Abcam
MRE11A	ChIP	600-401-872	Rockland
MRE11 A	WB, IF	SC-22767	Santa Cruz
NBS1/Nibrin	WB	sc-374168	Santa Cruz
PARP1	WB	H-250/ sc-7150	Santa Cruz
PAR = $(ADP\text{-}ribose)_n$	WB	10HA	Trevigen
HA-tag (hemagglutinin)	WB, IP, ChIP	F-7/ sc-7392	Santa Cruz
β-Actin	WB	A2228	Sigma-Aldrich
GAPDH	WB	6C5/ sc-32233	Santa Cruz

WB: western blot, IP: immunoprecipitation, IF: immunofluorescence, ChIP: chromatin IP

Table S3 si-RNAs and sh-RNAs used in this study

si- (or sh-) RNAs	species	Catalogue#	Vendor
Control si-RNA	any animal species	sc-37007	Santa Cruz
Control sh-RNA lentivirus vector	any animal species	sc-108060	Santa Cruz
BIN1 si-RNA	human	sc-29804	Santa Cruz
BIN1 sh-RNA lentivirus vector	human	sc-29804-SH	Santa Cruz
E2F1 si-RNA	human	sc-29297	Santa Cruz
E2F2 si-RNA	human	sc-29298	Santa Cruz
E2F3 si-RNA	human	sc-37817	Santa Cruz
ATM si-RNA	human	sc-29761	Santa Cruz
MRE11A si-RNA	human	sc-37395	Santa Cruz
NBS1 si-RNA	human	sc-36061	Santa Cruz

si-RNA: small interfering RNA, sh-RNA: short hairpin RNA

Table S4 Chemicals used in this study

Chemicals	Catalogue #	Vendor
Cisplatin	P4394	Sigma-Aldrich
Etoposide	E1383	Sigma-Aldrich
Bleomycin	B-2434	Sigma-Aldrich
RI-1 (RAD51 inhibitor)	553514	CalBiochem
KU-60019 (ATM inhibitor)	4176	Tocris Bioscience
4′-6-diamino-2-phenylindole (DAPI)	D8417	Sigma-Aldrich

Supplemental References

S1) Pyndiah, S., Tanida, S., Ahmed, K. M., Cassimere, E. K., Choe, C., and Sakamuro, D. (2011) c-MYC suppresses BIN1 to release poly(ADP-ribose) polymerase 1: a mechanism by which cancer cells acquire cisplatin resistance. Sci. Signal. **4**, ra19

S2) Lundgaard, G. L., Daniels, N. E., Pyndiah, S., Cassimere, E. K., Ahmed, K. M., Rodrigue, A., Kihara, D., Post, C. B. and Sakamuro, D. (2011) Identification of a novel effector domain of BIN1 for cancer suppression. J. Cell. Biochem. **112**, 2992-3001

S3) Routhier, E. L., Donover, P. S., and Prendergast, G. C. (2003) hob1+, the fission yeast homolog of Bin1, is dispensable for endocytosis or actin organization, but required for the response to starvation or genotoxic stress. Oncogene **22**, 637-648

S4) Golding, S. E., Rosenberg, E., Valerie, N., Hussaini, I., Frigerio, M., Cockcroft, X. F., Chong, W. Y., Hummersone, M., Rigoreau, L., Menear, K. A., O'Connor, M. J., Povirk, L. F., van Meter, T., and Valerie, K. (2009) Improved ATM kinase inhibitor KU-60019 radiosensitizes glioma cells, compromises insulin, AKT and ERK prosurvival signaling, and inhibits migration and invasion. Mol. Cancer Ther. **8**, 2894-2902

S5) Polyak, K., Xia, Y., Zweier, J. L., Kinzler, K. W., and Vogelstein, B. (1997) A model for p53-induced apoptosis. Nature **389**, 300-305

S6) Okazaki, T., and Sakamuro, D. (2007) Induction of Fas (CD95/APO-1) ligand is essential for p53-dependent apoptosis in an *in vitro* renal carcinoma model system. J. Cancer Res. Clinc. Oncol. **133**, 581-588